



CHALMERS
UNIVERSITY OF TECHNOLOGY

Chemical looping combustion (CLC) of municipal solid waste (MSW)

Downloaded from: <https://research.chalmers.se>, 2026-04-03 17:31 UTC

Citation for the original published paper (version of record):

Yaqub, Z., Oboirien, B., Leion, H. (2023). Chemical looping combustion (CLC) of municipal solid waste (MSW). *Journal of Material Cycles and Waste Management*, 25(4): 1900-1020.
<http://dx.doi.org/10.1007/s10163-023-01674-z>

N.B. When citing this work, cite the original published paper.



Chemical looping combustion (CLC) of municipal solid waste (MSW)

Z. T. Yaqub¹ · B. O. Oboirien¹ · H. Leion²

Received: 27 December 2022 / Accepted: 11 April 2023 / Published online: 12 May 2023
© The Author(s) 2023

Abstract

Chemical Looping Combustion (CLC) has been found to be a better alternative in converting Municipal Solid Waste (MSW) to energy and has the potential to reduce the generation of dioxins due to the inhibition of the de-novo synthesis of dioxins. This study comprehensively reviews the experimental studies of CLC of MSW, the oxygen carriers, reactor types, performance evaluation, and ash interaction studies. Modeling and simulation studies of CLC of MSW were also critically presented. Plastic waste is MSW's most studied non-biomass component in MSW under CLC conditions. This is because CLC has been shown to reduce the emission of dioxins and furans, which are normally emitted during the conventional combustion of plastics. From the several oxygen carriers tested with MSW's CLC, alkaline earth metals (AEM) modified iron ore was the most effective for reducing dioxin emissions, improving combustion efficiency and carbon conversion. Also, oxygen carriers with supports were more reactive than single carriers and $\text{CaSO}_4/\text{Fe}_2\text{O}_3$ and CaSO_4 in silica sol had the highest oxygen transport ability. Though XRD analysis and thermodynamic calculations of the reacted oxygen carriers yielded diverse results due to software computation constraints, modified iron ore produced less HCl and heavy metal chlorides compared to iron ore and ilmenite. However, alkali silicates, a significant cause of fouling, were observed instead. The best reactor configuration for the CLC of MSW is the fluidized bed reactor, because it is easy to obtain high and homogeneous solid–gas mass transfer. Future research should focus on the development of improved oxygen carriers that can sustain reactivity after several cycles, as well as the system's techno-economic feasibility.

Keywords Chemical looping combustion (CLC) · Municipal solid waste (MSW) · Oxygen carrier · Plastic waste · Dioxins

Introduction

The increase in the volume of MSW generated and the threat to the ecosystem has led to more research on effective ways to solve the issue of processing our waste streams [1]. MSW consists of plastics, paper, textiles, food waste, garden waste, wood, metal and glass, as seen in Fig. 1 [2]. As the world population increases with the increase in economic and industrial development, there will not be enough landfills to meet the population demand and the demand for energy will eventually outweigh the supply [3]. Waste-to-energy technology is believed to help manage our municipal solid waste due to its ability to reduce greenhouse gas emissions

and generate energy [4, 5]. An effective waste management system must be environmentally sustainable, viable and generally acceptable [6]. Improper waste management can spread pathogens [7], water contamination [8], and soil and air pollution [9].

Different solid waste management processes have been studied to dispose off MSW effectively. Landfilling is the most common waste disposal method, especially in developing countries. It is an open dumping system that can lead to air, water and land pollution [10]. Also, this waste management system has high maintenance, transport and labor costs [2]. MSW has a heating value ranging from 8.5 to 23 MJ/kg as analyzed in different literatures [2, 11–14] depending on the location, source and characterization, which makes it a good source of fuel for transportation, power generation and in powering equipment in petrochemical industries. Incineration, which is a type of thermal conversion and a source of energy that involves combusting solid waste at a high temperature in excess oxygen, has a lot of challenges which include high operating costs [15], corrosion of the

✉ B. O. Oboirien
boboirien@uj.ac.za

¹ Department of Chemical Engineering Technology,
University of Johannesburg, Johannesburg, South Africa

² Department of Chemical and Biological Engineering,
Chalmers University of Technology, Göteborg, Sweden

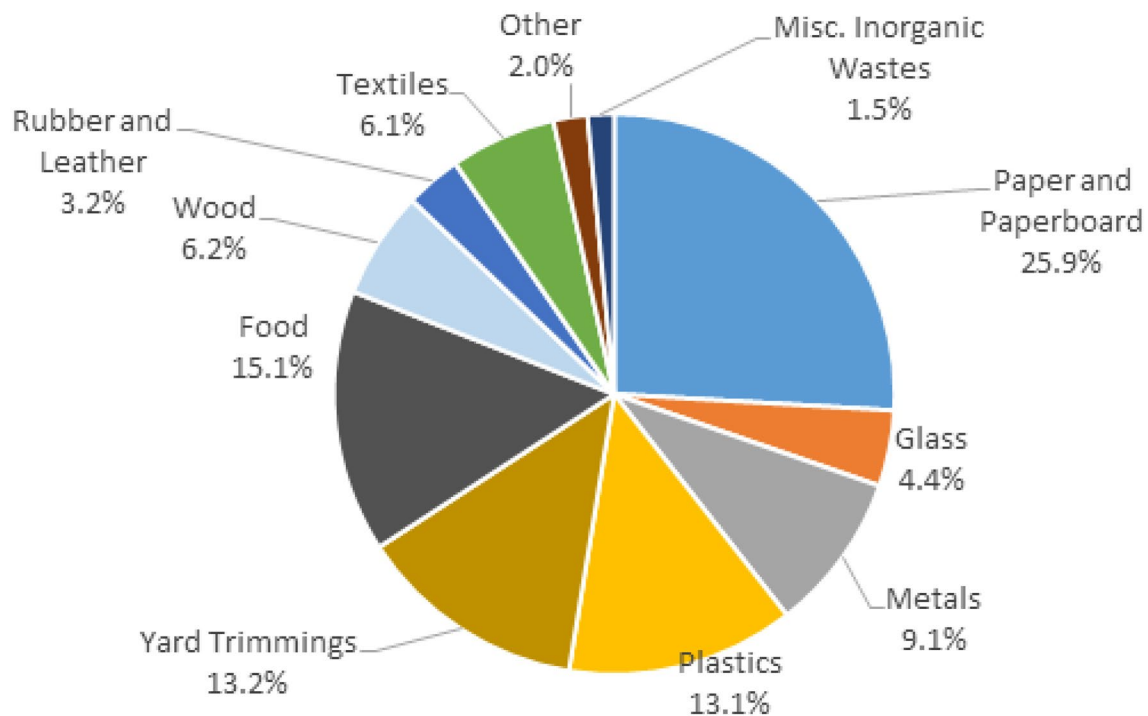


Fig. 1 Total MSW generated, 2015 [120]

combustion chamber [16], boiler fouling and presence of heavy metals and dioxins in incineration gasses [16].

Wang et al. [17] carried out a heavy metal analysis on the fly ash produced from the combustion of MSW in China and found that it contains large quantities of As, Cd, Cr, Cu, Ni, Pb, Zn, and Hg. The soils in the vicinity of the incineration plants were also tested and found to contain significant traces of these heavy metals [18]. Gabbar et al. [16] reviewed major heat treatment methods for MSW and discovered that landfilling and combustion are incompatible with the growth rate of MSW per year. Furthermore, while the combined pyrolysis-gasification process has the highest capital, operating and maintenance costs for MSW, it also has the lowest environmental impact [16].

Due to the challenges presented above from the different thermal methods of converting waste to energy, chemical looping combustion (CLC) has been found to be a better alternative in converting waste to energy and has the potential to reduce the generation of dioxins due to the inhibition of the de-novo synthesis of dioxins [19]. Chen et al. [20] reported that reducing chlorine and other heavy metal emissions is possible when a suitable oxygen carrier is selected. Chemical Looping combustion is a relatively new high-efficiency carbon capture and storage (CCS) technology that also proffers solutions to the high greenhouse gas emission by capturing CO₂ with low energy demand and cost penalty. Since CO₂ concentrations in the atmosphere have risen sharply in recent decades as a result of the

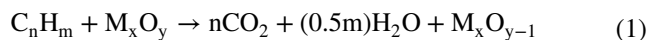
world's reliance on fossil fuels for energy production, and global atmospheric CO₂ concentrations have risen from 280 to 390 ppm [21] in the early twenty-first century and has exceeded 400 ppm in current times [22] and projected to be between 550 and 970 ppm at the end of the century [23]. CLC has been developed to produce a concentrated stream of CO₂ from industrial sources, transport it to a suitable storage location, and then store it away from the atmosphere for an extended period.

Presently, there is no comprehensive review that reports on CLC of MSW. This study comprehensively reviews the experimental studies of CLC of MSW, the oxygen carriers, reactor types, performance evaluation, and ash interaction studies. Modeling and simulation studies of CLC of MSW were also critically presented. Finally, research gaps were identified for future research directions.

Description of the CLC process

Lewis and Gilliland developed and patented a concept very similar to chemical looping combustion in 1954 [25]. The patent, titled “production of carbon dioxide,” described the reduction of oxygen carriers in two interconnected fluidized beds using various fuels. The key of the process is that the oxygen used is derived from a metal oxide (M_xO_y) and serves as an oxygen carrier [26].

The combustion process occurs in two interconnected reactors: the fuel and air reactor. The fuel reacts with the oxygen carrier in the fuel reactor to produce CO_2 and steam gases (reduction, reaction 1). The CO_2 -rich flue gas undergoes condensation and purification to achieve a highly concentrated CO_2 that is transported for storage [27]. While in the air reactor, the reduced oxygen carrier (M_xO_{y-1}) reacts with air and oxidizes to its original form (oxidation, reaction 2). Figure 2 shows the schematic diagram of a CLC of solid fuel with a $\text{Cu}_2\text{O}/\text{CuO}$ oxygen carrier [28]. The heat required during the reduction process in the fuel reactor can be supplied from the air reactor during the oxidation reaction [29]. Since the CO_2 produced is captured, no energy penalty is involved in separating the combustion gases [30]. Hence, the estimated cost of CO_2 sequestration in CLC (20 US\$/ ton of CO_2 isolated from the atmosphere) is less than that of other clean combustion technologies (between 28 and 67 US\$/ ton of CO_2 in pre-combustion, post-combustion and oxyfuel combustion) [31]. The sum of the reactions that take place in the fuel and air reactors is equal to the net combustion reaction (reaction 3)



CLC process can have different reaction pathways for fuel conversion irrespective of the type of fuel used. In situ Gasification CLC (iG-CLC) occurs when fuel is gasified in the fuel reactor and the gaseous combustibles react directly with the oxygen carrier. This is the most common pathway for CLC. The other reaction pathway is the Chemical-Looping with Oxygen Uncoupling (CLOU) process which relies on the use of oxygen-carrier materials that release gaseous oxygen in the fuel reactor, allowing the solid fuel to burn with gas-phase oxygen [32]. Although the best reaction pathway is determined by the type of fuel, fuel gas concentration, reaction temperature and the reactivity of the oxygen carrier [33], however, Leion et al. [34] concluded that a higher char conversion rate is obtained from the CLOU process than that of the in situ gasification CLC process when copper oxide was used as an oxygen carrier for different types of coal, coke and wood char fuel.

CLC has been tested with different fuels; gaseous fuels (natural gas [35], methane [36], refinery gas or off-gas from steam reforming [36]), solid fuels (coal [37], biomass [38], petroleum coke [21] and other solid wastes (waste paper, plastics, etc.) [39]) and liquid fuels such as heavy oils [40]. As described by Wang et al. [28], for solid fuel CLC, the fuel undergoes a devolatilization process which releases volatiles and char. Simultaneously, the volatiles reacts with the oxygen carrier, and the char (mainly carbon) undergoes syngas gasification with steam and/or CO_2 to produce syngas (reaction 4 and 5). With steam as a gasification agent, a water–gas shift reaction also occur to produce H_2 and CO_2 gasses [41]. The intermediate gasification product then reacts with the oxygen carrier to produce an enriched CO_2 stream [42]. Although steam gasification has a higher gasification rate, the cost of generating steam is very high, which inherently increases the cost of CO_2 capture [43]. Due to this reason, Adanez et al. [44] suggested that the CO_2 from the flue gas after steam condensation can be partly recycled to the fuel reactor as part of the gasification reaction to reduce the amount of steam used for gasification, as seen in Eq. 5. The reduced oxygen carrier from the fuel reactor is then transferred to the air reactor, where it is re-oxidized by oxygen from air. In CLC systems, solid waste has been found to have higher overall reactivity than coal, and its char allows for faster complete burnout [45]. It also has a lower potential for carbonaceous material transfer to the metal/air reactor, where it would burn and emit CO_2 .

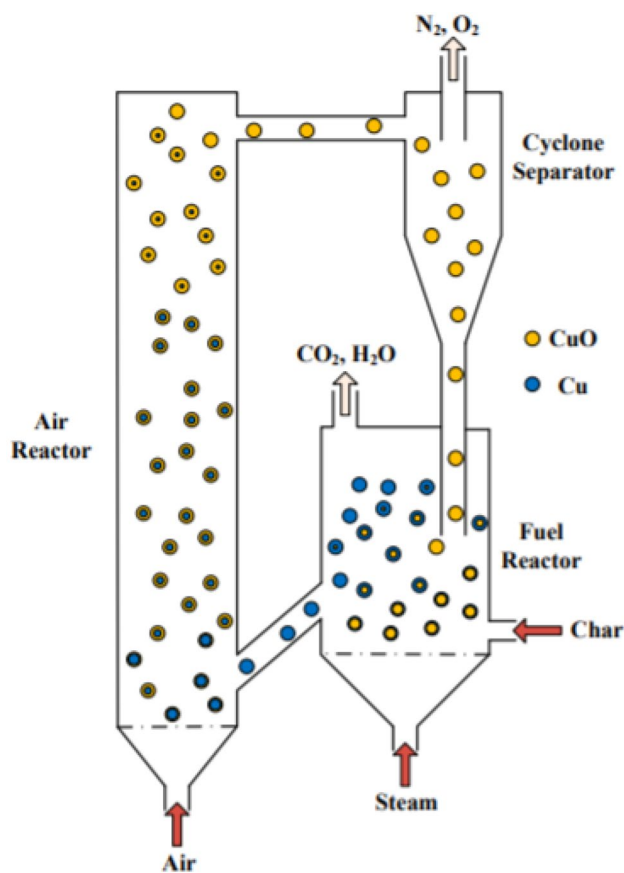
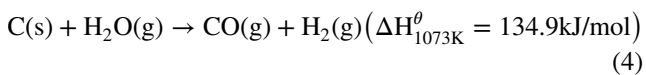


Fig. 2 Example of a CLC configuration [28]



Experimental studies of CLC of MSW

IG-CLC and CLOU experiments have been tested for different solid fuels (coal [45] and biomass [46, 47]) on a pilotscale years before the first experiment for MSW was published and has been found to be a promising technique. However, scaling up the process is quite challenging due to its low fuel conversion and CO₂ concentration in the fuel reactor. The unsatisfactory fuel conversion rate was caused by the disparity between the rate of char gasification reaction and the combustion reaction between the gasification products and oxygen carriers [48]. At the same time, the low CO₂ concentration in the fuel reactor is caused by the poor gas–solid interaction, agglomeration of the oxygen carrier particle cluster, etc., in the fluidized bed reactor [49].

The first experiment on CLC of MSW was published in 2006 by Cao et al. [50], where different solid fuels (coal, biomass and low-density polyethylene MSW) were compared based on their redox kinetics using copper oxide (CuO) as an oxygen carrier. The authors used wood and low-density polyethylene (PE) to study the performance of biomass and MSW. They concluded that MSW with high volatile contents showed excellent promise in the development of the chemical looping combustion process. Table 1 summarizes different CLC experiments for MSW from 2006 to date. The table also presents the types of reactors used, oxygen carriers, objective and the inference observed from the experiments. Another type of waste that has been analyzed for the CLC process is biomass waste. Comparing different biomasses that have been analyzed, woodchips and sawdust had a high CO₂ capture rate of > 90% [51] and a reduction in NO of up to 30% [52]. However, the aggressive ash in the samples is a difficulty with biomass waste. Pine sawdust contains 41% ash, with potassium being the most problematic key component [53]. On the other hand, this review will concentrate on non-biomass MSW, a relatively new solid fuel tested for CLC. Plastic waste is MSW's most commonly studied non-biomass component in MSW under CLC conditions [19, 54]. This is because CLC has been shown to reduce the emission of dioxins and furans, which are normally emitted during the conventional combustion of plastics [55].

Different types of MSW studied under CLC conditions

As mentioned earlier, plastic wastes are the most common type of MSW studied under CLC conditions. These have

been investigated in order to determine the fate of heavy metals present in plastic waste (such as cadmium and chromium), the emission of dioxins formed from the presence of chlorine in plastics, and their reaction performance with various oxygen carriers. Plastic wastes such as polyvinylchloride (PVC) [54, 56], polyethylene [50], polyurethane, and polypropylene [57] have been experimentally investigated under CLC conditions. A process simulation of CLC of various plastic wastes (polypropylene, polyethylene terephthalate, polystyrene, high-density polyethylene and low-density polyethylene) was performed by Yaqub et al. [58] and predicted their performance based on their CO₂ yield and combustion efficiency. Wang and Zhao [59] and Ma et al. [60] used a medical perfusion tube whose properties are similar to PVC for the CLC process. Other kinds of MSW investigated for the CLC process include pyrolysis gas-derived PVC waste [55], pyrolysis gas-derived MSW [61], syngas-derived MSW [62], bottom ash from MSW [63] and waste paper [39]. MSW blends (waste paper and different plastics) [64] and a mixture of flour, paper, sawdust, cotton cloth, polystyrene, inert materials and non-combustible MSW to represent actual MSW [20] were also studied to evaluate the reaction performance and heavy metal transformation in the CLC process. Due to the heterogenous characteristics of MSW, the components of the solid waste are individually analyzed or a mixture of components with similar properties except for Chen et al. [20], where MSW of different properties were used. Although the authors did not mention the challenge faced with using the combination of the different MSW components, however, Strohle [24] believes combining the solid waste of different properties will lead to varied volatiles released which subsequently leads to varied gas composition at the outlet of the fuel reactor and incomplete conversion of the volatiles and gasification products. Nevertheless, solutions such as the addition of oxygen produced from an air separation unit to a post-oxidation chamber can be deployed.

Another effective solution deployed by Hakandai et al. [65] is the hydrothermal treatment of the MSW prior to CLC, a form of pretreatment method. This process ensures the powdered MSW produced has a higher material uniformity and a higher carbon content and calorific value. This modification is also necessary to fit into the reactor to be used for the CLC process. Other pretreatment methods include but are not limited to sorting, leaching and mechanical size reduction. The capital cost for this pretreatment method is usually moderate and worth its benefit.

Reactors' configurations used for CLC of MSW

The CLC process can be carried out in different reactor configurations based on different reactor designs. It can be configured as two interconnected moving or fluidized reactors,

Table 1 Summary of different experiments performed on CLC of MSW

S/N	Year	Objective	Type of MSW	Type of reactor	Oxygen carrier	Observations	References
1	2006	Test the reduction property of oxygen carrier on solid waste	Polyethylene (PE)	Micro-reactor	CuO	Solid waste is desirable for the development of the CLC process	[55]
2	2013	To study the effect of the oxygen carrier on the combustible waste	Combustible municipal solid waste	Two-stage tubular reactor	Copper-based oxygen carrier	The oxygen carrier had a high mechanical strength and excellent reaction and recycle stability	[56]
3	2014	Feasibility of an annular dual tube moving bed reactor for CLC	Polypropylene (PP) and polyurethane (PU)	annular dual tube moving bed reactor for CLC	alumina-supported Fe ₂ O ₃ (Fe ₂ O ₃ /Al ₂ O ₃) with 60 wt.% Fe ₂ O ₃	100% of PU and PP conversion was reached through moving bed operation	[50]
4	2015	To investigate the reaction of PVC pyrolysis gas and calcium-based oxygen carrier	PVC	Two-stage reactor	CaSO ₄ /Fe ₂ O ₃	Addition of Fe ₂ O ₃ in CaSO ₄ increases the reaction rate	[57]
5	2015	To study the formation of PCCDF's in CLC of PVC	PVC	Tubular furnace	CaSO ₄ in silica sol	A reduced dioxin yield and international toxic equivalence quantity (I-TEQ) were observed when compared with conventional incineration	[58]
6	2016	Comparing the reactivity of Cao-decorated Fe ₂ O ₃ /Al ₂ O ₃ with Fe ₂ O ₃ /Al ₂ O ₃	Medical plastic waste	Fluidized bed reactor	CaO-decorated Fe ₂ O ₃ /Al ₂ O ₃	CaO decoration resulted in lower reactivity of the oxygen carrier	[24]
7	2017	Comparison of conventional incineration with CLC of plastic waste	Plastic wastes	Fluidized bed reactor	Cao-decorated Fe ₂ O ₃ /Al ₂ O ₃	A more significant inhibition of dioxins in CLC than in conventional incineration	[59]
8	2018	To determine the performance of the oxygen carrier (dioxin emission)	Plastic waste	Semi-continuous fluidized bed reactor	Natural iron ore with CaO adsorbent	The oxygen carrier was able to suppress the formation of chlorobenzene, an intermediate of dioxin and did not deteriorate the performance of the oxygen carrier	[52]
9	2019	Transformation and migration properties of cadmium	Synthetic MSW (flour, paper, sawdust, cotton cloth, polystyrene and inert materials)	Tubular furnace	Copper and iron-based oxygen carrier	Cadmium present in MSW can be effectively removed from the CLC process	[25]
10	2020	Test the redox performance of iron-modified oxygen carrier	MSW derived syngas	Batch fluidized bed reactor	Iron ore modified with barium aluminate (BaAl ₂ O ₄)	Significant improvement in the reactivity of the iron ore the rate of reaction of the iron ore were significantly improved with the introduction of barium aluminate	[60]
11	2020	To compare the performance of different waste fuel	Waste paper and plastic	Fluidized bed reactor	Ilmenite	The waste paper had a higher fractional conversion to CO ₂ due to the high volatiles present in the solid fuel	[42]

Table 1 (continued)

S/N	Year	Objective	Type of MSW	Type of reactor	Oxygen carrier	Observations	References
12	2020	Improving the redox performance of iron ore	MSW-derived syngas	Fluidized bed reactor	Iron ore modified with alkaline earth metal (AEM)	Increased reactivity of the modified oxygen carrier and increased sintering resistance	[61]
13	2021	To study the fate of zinc, copper and lead in CLC of waste fuel	A mixture of municipal solid waste and industrial waste	Circulating fluidized bed (CFB) boiler	Ilmenite	Copper and lead were found to react with the ilmenite to form ferrites, and lead was condensed to lead chloride in the fly ash	[62]
14	2021	Reducing the H ₂ S emission from MSW	MSW derived syngas	Fluidized bed reactor	Iron ore modified with AEM (BaO, CaO, MgO)	BaO improves the performance of the iron oxide Cao and MgO were ineffective in sulfur removal from MSW-derived syngas	[63]
15	2022	To determine the dechlorination performance of CLC of plastic wastes	Polyvinyl chloride	Fixed bed reactor	Iron ore decorated with aluminum earth metals (K, Na and Ca)	The modified iron ore improved the performance of the OC and high dechlorination efficiency	[64]
16	2022	To determine the thermal behavior of oxygen carrier with CLC of MSW-derived syngas	MSW derived syngas	Fluidized bed reactor	Mg–Al-supported composites of CuO Oxygen carrier (OC) and Ba/Sr sorbent	The CuO/Cu migration to the surface enhanced the stability on mechanical strength, elemental composition and redox ability maintaining the stability in the reactivity with MSW syngas for long-term operation	[65]

packed or fluidized bed reactors, bubbling bed reactors and rotating reactors. The bubbling bed reactor also has a high solid inventory which is beneficial for high char conversion [43]. Most CLC setups have two loop seal devices usually placed between the reactors and the cyclone to prevent gas mixing between the two reactors [66].

For the CLC of MSW, the key reactor configuration investigated are (a) annular dual-type moving bed reactor, (b) dual batch fluidized bed [62], (c) semi-continuously operated fluidized bed [60], (d) two-staged pipe reactor [56] (e) gas-switching fluidized bed reactor [67] (f) fixed bed reactor setup [55] (g) fixed bed reactor system [20] (h) fluidized bed reactor [68]. The schematic diagram of these reactors is presented in Fig. 3.

Most of the CLC experimental reactor design used for MSW consists of single stage reactors except for Bi et al. [56] and Wang et al. [69], where two tubular reactors and two batch fluidized bed reactors were used, respectively. The tubular reactors used by Bi et al. [56] represented the fuel and air reactors. Nitrogen was used as the fluidizing gas in this experimental setup. However, for Wang et al., [69], two sets of tests were conducted simultaneously in the fluidized bed reactors. Reduction, purging and oxidation occurred in the reactors with water at 150 °C introduced as a gasification agent during the reduction process. Purging was done by introducing pure N₂ into the system to avoid contact with the oxidation and reduction gases.

Ma et al. [60] used a semi-continuously operated fluidized bed reactor. The interconnected fluidized bed reactor was the most commonly used configuration [70]. The interconnected fluidized bed reactor configuration continuously introduces the OC and plastic waste into the reactor via two screw feeders. The two screw feeders' rotation speeds can be precisely controlled to determine the feeding rate of plastic waste (corresponding to thermal power) and the feeding rate of fresh OC. The fluidizing gas used H₂O and N₂ gas, similar to what was used by Wang and Zhao [19], Liu et al. [67] and Yaqub et al. [39] for the laboratory scale batch fluidized bed reactor for CLC of plastic waste and waste paper. The fluidized bed reactor ensures good mixing of the gas and solid carrier and easy circulation and replacement of the carrier material [71]. The solid particles leaving the reactors are recovered by a cyclone and sent back to the fuel and air reactor [30].

The moving bed reactor with an annular dual tube was used by Chiu et al. [57] for the CLC of PP and PU. In this setup, there are two solid inlets for the MSW and the oxygen carrier, designed as a screw conveyor for easy access into the reactor. O₂ and CO₂ were used as the gasification agent for the PP and PU MSW samples. The moving bed fuel reactor was attractive in maintaining complete fuel conversion and maximizing solid conversion [72]. Jiang et al. [58] used a fixed bed reactor to determine the dechlorination performance of PVC plastic waste. Apart from the

main reactors in CLC, other components such as cyclones (to separate the entrained particles from the fuel reactor and air reactor), preheaters (to preheat air and fluidization gases) and filters (to further purify the CO₂ gas leaving the reactor) are added to the CLC setup. While preheaters and filters are necessary for all setups, not all have cyclones attached to them.

Also, since the reaction in the air reactor is highly exothermic during reoxidation of the oxygen carrier, excess heat can serve as a by-product and can be used for steam evaporation, preheating of air and fluidization gases even in the CLC setup thereby reducing the operating cost of the system. The CLC setup can also be integrated with another unit process to produce suitable by-products such as hydrogen and methanol to increase the economic revenue of the system. Hakandai et al. [65] introduced a methanol synthesis reactor to convert the CO₂ and H₂ produced from the CLC process to methanol and a combined cycle process for power generation. The process has been found to be feasible and competitive. Also, Miyahira and Aziz [73] integrated the Haber–Bosch process for NH₃ synthesis into the syngas chemical looping process of agricultural waste (rice husk) to produce ammonia which is utilized as agricultural fertilizer. Although the integration of the two processes shows a high energy efficiency, its economic viability has not been established.

For other solid fuels such as coal and biomass tested with the CLC process, the configuration of two interconnected fluidized-bed reactors with thermal inputs ranging from 0.5 kWth to 3 MWth have been built and operated [74]. In addition, a 25 kWth CLC unit with solid fuels was developed, with a moving bed as the fuel reactor and an entrained bed as the air reactor [75]. The three main types of bed reactors used for other solid fuels, as reviewed by Song and Shen [45], are bubbling bed, spout fluidized bed, and circulating bed due to their high char conversion and lower oxygen carrier requirements. These reactors are similar to what is operated for MSW.

Oxygen carriers reported in the CLC of MSW

The development of oxygen carriers is a significant challenge in the CLC process. An effective oxygen carrier must have the ability to do the following [76]:

- High mechanical strength
- Environmentally friendly
- Cheap
- Sufficient oxygen transport capacity
- Good thermodynamic properties for fuel conversion
- Highly reactive during the oxidation and reduction reaction

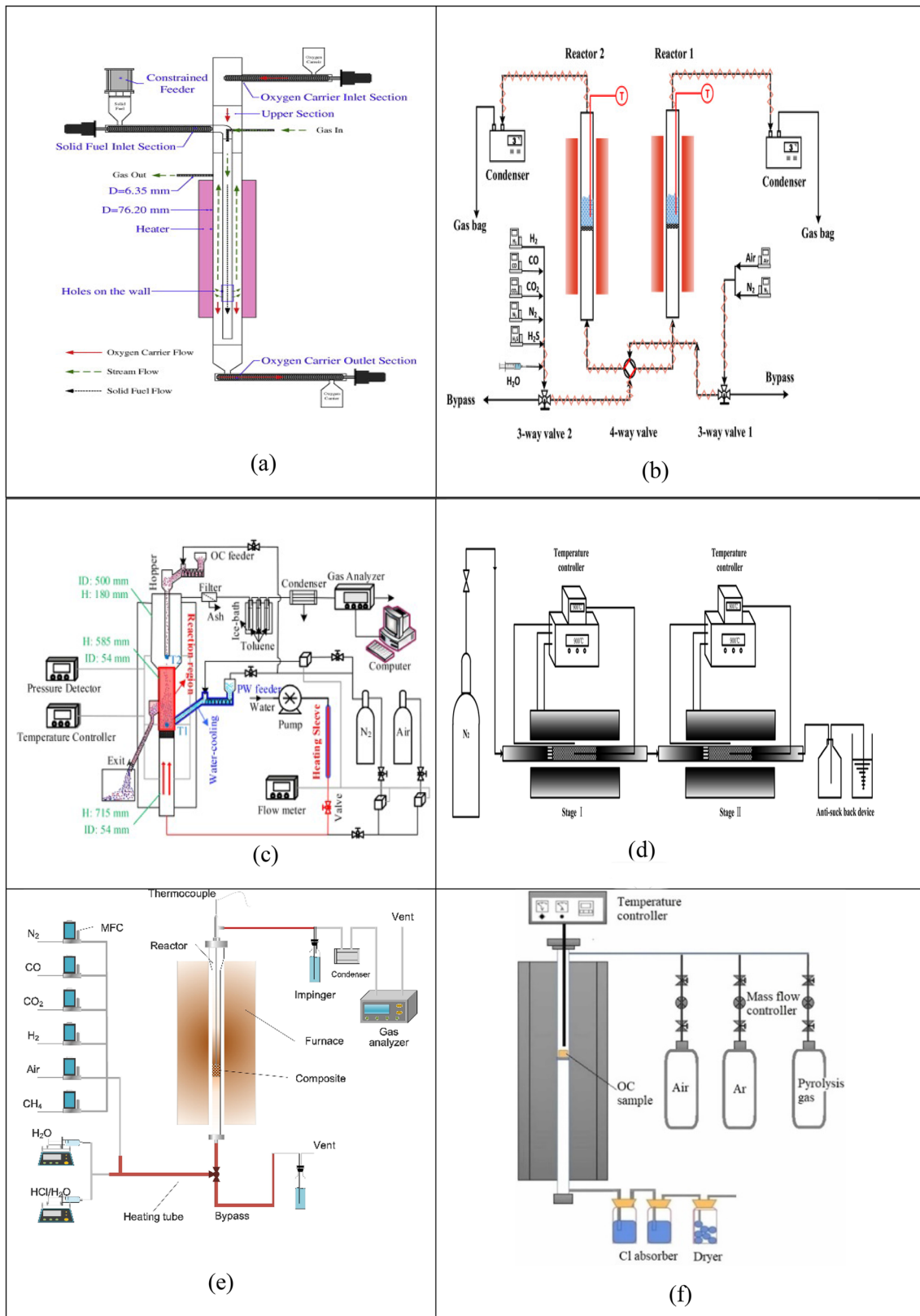
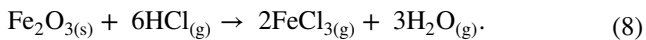
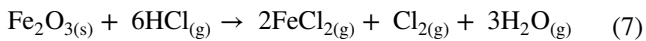


Fig. 3 Reactor configurations tested with CLC of MSW **a** Annular dual-type moving bed reactor **b** Dual Batch fluidized bed [62] **c** semi-continuously operated fluidized bed [60] **d** two-staged pipe reactor

e gas-switching fluidized bed reactor [67] **f** fixed bed reactor setup [55] **g** fixed bed reactor system [20] **h** fluidized bed reactor [68]



For oxygen carriers with supports, Chiu et al. [57] used an iron-based oxygen carrier (Fe_2O_3) supported with alumina (Al_2O_3). This oxygen carrier is believed to enhance the utilization of oxygen present in the oxygen carrier when used with a moving bed reactor [87]. Combining this oxygen carrier with an annular dual-type moving bed reactor was able to achieve a complete carbon conversion at an oxygen carrier to fuel ratio of 1.86 and 6.56 for polyurethane and polypropylene, respectively.

Furthermore, 85 wt% iron ore (Fe_2O_3) with different alkaline earth metals in the form of oxides and aluminates (BaO , CaO , MgO , BaAl_2O_4 , CaAl_2O_4 and MgAl_2O_4) were used as oxygen carriers for CLC of MSW-derived syngas to improve the reactivity of the iron ore. Based on the TGA, CLC performance evaluation in the batch fluidized bed reactor and the XRD analysis, the BaO support was found to have the best performance and highest lattice oxygen reactivity [62]. Another Fe_2O_3 supported with CaSO_4 oxygen carrier was analyzed by Bi et al. [56]. This oxygen carrier was found to have a good heat stability at a temperature of 900 °C and complete conversion of the PVC pyrolysis gas was obtained at a fuel-to-oxygen carrier mass ratio of 8.

Experimental evaluation of the performance evaluation of CLC of MSW

The three main combustion performances which are usually analyzed with CLC of MSW are the oxygen carrier performance (oxygen demand), CO_2 capture and fuel conversion. The oxygen demand Ω_n is the ratio of the oxygen required to oxidize the unburnt gas leaving the fuel reactor to CO_2 and H_2O to the total oxygen required to oxidize the gas released from the fuel in the fuel reactor [88]. CO_2 capture η_{CO_2} is the ratio of the gaseous carbon leaving the fuel reactor to the total carbon converted to gas in the fuel reactor [89]. The fuel conversion η_F is the ratio of the carbon converted to gaseous compound in the air and fuel reactor to the total carbon added [31].

Reactivity of oxygen carriers

One of the main objectives of the CLC of MSW is to reduce the amount of choline emitted during the combustion process, which was found to produce dioxins, a persistent organic pollutant. Due to this, oxygen carriers have been modified to meet this demand. The redox performance of these oxygen carriers has been evaluated by different authors using

thermogravimetric analysis (TGA) in order to determine the reactivity of the lattice oxygen present in the oxygen carrier.

Wang et al. [62] compared the mass loss rate of different modified oxygen carriers to determine the most reactive. Iron ore (IO) modified with alkaline earth metal (AEM) oxides (BaO , CaO , and MgO) and alkaline earth metal aluminates (BaAl_2O_4 , CaAl_2O_4 , and MgAl_2O_4) were compared using MSW-derived syngas as fuel. The analysis showed that the AEM oxides had better reactivity than the AEM aluminates. The iron ore modified with Barium oxides (BaO) showed the best performance in improving the iron ore activity. Also, iron ore doped with HCl sorbent was analyzed to determine the oxygen carrier's reactivity for HCl removal from MSW-derived syngas. The author observed that the iron ore without the doping could not efficiently remove the HCl due to an unfavorable thermodynamic reaction between the Fe_2O_3 and HCl [90]. In general, the Ba alkaline earth metal showed the highest reactivity, followed by Ca, then Mg when modified with iron ore.

Similarly, modified AEM with $\text{CuO-Al}_2\text{O}_3$ was also analyzed at different weight ratios by Liu et al. [91]. Except for that with barium, the other modified oxygen carriers had a better oxygen transport capacity. In essence, barium oxide or aluminate has a better oxygen transport capacity when mixed with iron oxide than copper oxide.

Other modified oxygen carriers that have undergone TGA analysis to determine their reactivity for CLC of MSW include pure CaSO_4 , CaSO_4 in silica sol and $\text{CaSO}_4/\text{Fe}_2\text{O}_3$ [54, 56], $\text{CaO/K}_2\text{O/Na}_2\text{O}$ adsorbents on $\text{Fe}_2\text{O}_3/\text{Al}_2\text{O}_3$ and pure $\text{Fe}_2\text{O}_3/\text{Al}_2\text{O}_3$ [92]. In both cases, the modified oxygen carriers were found to have a higher reaction rate than the pure oxygen carriers. However, the $\text{CaO/K}_2\text{O/Na}_2\text{O}$ -decorated $\text{Fe}_2\text{O}_3/\text{Al}_2\text{O}_3$ hinders the transfer of active lattice oxygen in OC particles. This could be due to the modified oxygen carrier's larger surface area, which impedes the contact of the oxygen carrier with the reactants. Alkali metal oxides such as BaO modified with the $\text{Fe}_2\text{O}_3/\text{Al}_2\text{O}_3$ give a better reactivity, as analyzed by Wang et al. [62].

The oxygen transport capacities of some modified oxygen carriers used for CLC of MSW are summarized in Table 2. Compared to modified oxygen carriers, the oxygen transport capacity of pure metal oxides is from 0.01 to 0.2 [93]. In summary, CaSO_4 and oxygen carriers mixed with CaSO_4 have the best oxygen transport capacity and are highly reactive. However, this oxygen carrier has a low regeneration ability of about 64.6% after just six cycles due to possible side reactions during oxidation to produce CaO (reactions 9–12)

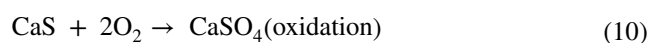
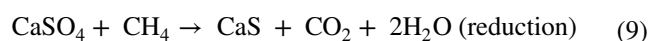
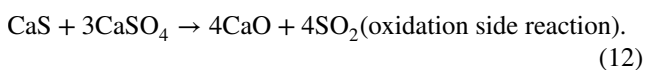
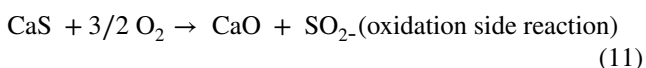


Table 2 Summary of the oxygen transport capacity of different oxygen carriers analyzed with TGA

Oxygen carrier	Composition ratio	Oxygen transport capacity (%)	References
CaSO ₄ —Silica sol	87:14	41	[58]
CaSO ₄	100	~45	[57]
CaSO ₄ —Fe ₂ O ₃	95.2:4	~49.8	
CuAl	40:60	8.16	[100]
	30:70	6.19	
CuAlSr	40:50:10	8.45	
	30:60:10	6.3	
CuAlBa	40:50:10	7.76	
	30:60:10	5.6	
CuAlCa	40:50:10	8.66	
	30:60:10	6.56	
	40:55:5	8.46	
	40:40:20	9.25	
	40:30:30	9.63	
Fe-oxide	89.19	9.6	[62] ^a
Fe-oxide-BaO	83.7:6.25	22.1	
Fe-oxide-CaO	86.88:6.15	19.5	
Fe-oxide-MgO	84.49:5.47	9.6	
Fe-oxide-BaO-Al ₂ O ₃	86.49:3.53:2.88	16.8	
Fe-oxide-CaO-Al ₂ O ₃	86.45:2.72:3.47	14.5	
Fe-oxide-MgO-Al ₂ O ₃	88.86:1.01:3.07	10.2	

^aOnly active components are presented. Other components such as SiO₂ and TiO₂ were excluded



Combustion efficiency

Combustion efficiency is another performance parameter that can be used to measure the reactivity of the oxygen carriers. For most CLC of MSW experiments, the combustion efficiency was compared for various oxygen carriers. Wang et al. [62] compared the iron ore modified with AEM oxides and aluminates based on their CO and H₂ combustion efficiencies for CLC of MSW-derived syngas. While a higher CO combustion efficiency was obtained compared to the H₂ combustion efficiency due to the weaker bond strength of H₂ [94], the modified oxygen carriers had a higher combustion efficiency in the range of 80–100% and that of plain iron ore in the range of (45–75%). In conclusion, iron ore modified with the AEM oxides showed higher combustion efficiency for MSW-derived syngas than that with the AEM aluminates due to their stronger interactions with the iron oxide and the more stable properties of the aluminate [95].

However, a different trend was observed for the CLC of plastic waste by Wang and Zhao [92]. The combustion

efficiency when plain iron ore was used was higher than that of the different modified iron ore used. The authors believed it could either be due to diffusion limitations in the experiments or the adsorbent decoration hindering the transfer of active lattice oxygen. Other factors such as decoration methods and temperatures, were also compared to determine the best combustion efficiency. The physical mixture decoration method showed the best combustion efficiency compared to wet precipitation and coprecipitation methods. And the lowest temperature of 850 °C had the highest combustion efficiency. It should, however, be noted that even the lowest efficiency was greater than 90%. The authors also compared the CLC process (using the undecorated iron ore) with the conventional incineration method, and a higher combustion efficiency was observed with the conventional incineration [68]. The plastic waste CLC process produced a combustion efficiency greater than 90%, which means it is equally able to attain a highly efficient energy utilization.

Other factors such as the volume flow rate of the fluidizing agent, the mass flow rate of the oxygen carrier and the effect of Cao decoration were analyzed by Ma et al. [60] to evaluate the combustion efficiency of CLC of plastic waste. Using the CaO-decorated iron ore, oxygen carrier generally resulted in a combustion efficiency greater than 90%. Increasing the volume flow rate of the fluidizing agent reduced the combustion efficiency, while increasing the

mass flow rate of the oxygen carrier increased the combustion efficiency. This is because the higher superficial fluidization velocity means less bed inventory; thus, less active oxygen was provided [19].

CO₂ yield

The CO₂ yield is the ratio of CO₂ concentration to the total carbon concentration in the FR flue gas. A high CO₂ concentration in the concentration profiles signified a relatively high CO₂ yield. However, the mass flow rate of the oxygen carrier, fluidizing velocity and the volume flow rate of the fluidizing agent could also affect the CO₂ yield. While increasing the fluidizing velocity reduces the residence time, which leads to a reduced CO₂ yield from 97.8 to 97.2%, increasing the mass flow of the oxygen carrier and the fluidizing steam increases the CO₂ yield from 85 to 98% [19, 60].

For PU and PP plastic waste, an optimum oxygen carrier to fuel ratio of 1.86 and 6.56, respectively, was found to give an almost 100% CO₂ yield when an alumina-supported iron-based oxygen carrier was used in the CLC experiment [57]. The higher oxygen carrier flow rate used in PP is due to the higher carbon and hydrogen in PP plastic waste. In conclusion, the increased CO₂ concentration and low CO and CH₄ obtained in the concentration profile signify a high CO₂ yield for the CLC of MSW.

Carbon conversion

Carbon conversion is the measure of the mole of carbon in the flue gas to the mole of carbon added to the reactor. In other words, any residual char combustion in the air reactor will reduce the amount the carbon conversion in the CLC system. The use of CaO decorated and/or alumina-supported iron ore for CLC of the medical perfusion tube [19], PP and PU plastic waste [57] resulted in a high carbon conversion (80–98%). Hence, a sufficient oxygen carrier must be used to completely convert all the carbon present in the waste sample to obtain an almost complete carbon conversion. However, when ilmenite was used as an oxygen carrier for PVC plastic waste, carbon conversion of about 50% increased to approximately 85% when the temperature increased from 800 to 950 °C [39]. Also, the same authors used waste paper as a fuel and carbon conversion greater than 90% was obtained. The increase in carbon conversion is attributed to the high volatile content in waste paper compared to PVC waste. The increase in carbon conversion, temperature, mass flow rate of oxygen carrier and modified oxygen carrier with the ability to transport lattice oxygen was found to be the significant factors affecting the carbon conversion. Adanez et al. [31] and Ma et al. [60] analyzed all these operating parameters.

The maximum conversion rate, another performance tool analyzed, is similar to the carbon conversion and measures the gasification rate per unit of the non-gasified carbon in the

Table 3 Summary of oxidation and reduction phase characterization in different oxygen carriers analyzed with MSW

Before CLC	After CLC (Reduction)	After CLC (oxidation)	References
Fe ₂ O ₃ , SiO ₂	Fe ₃ O ₄ , FeO, SiO ₂	Fe ₂ O ₃	[61, 63]
Fe ₂ O ₃ , SiO ₂ , BaAl ₂ O ₄	Fe ₃ O ₄ , SiO ₂ , BaAl ₂ O ₄	–	
Fe ₂ O ₃ , SiO ₂ , CaAl ₂ O ₄	Fe ₃ O ₄ , SiO ₂ , CaAl ₂ O ₄	–	
Fe ₂ O ₃ , SiO ₂ , MgAl ₂ O ₄	Fe ₃ O ₄ , SiO ₂ , MgAl ₂ O ₄	–	
Fe ₂ O ₃ , SiO ₂ , BaCO ₃	Fe ₃ O ₄ , SiO ₂ , BaFe ₁₂ O ₁₉	Fe ₂ O ₃ , BaFe ₁₂ O ₁₉	
Fe ₂ O ₃ , SiO ₂ , CaO, Fe ₂ CaO ₄	Fe ₃ O ₄ , SiO ₂ , CaFe ₃ O ₅	Fe ₂ O ₃ , CaFe ₂ O ₄	
Fe ₂ O ₃ , SiO ₂ , MgO	Fe ₃ O ₄ , SiO ₂ , Mg _{1-x} Fe _x O	Fe ₂ O ₃ , MgFe ₂ O ₄	
CuO, MgAl ₂ O ₄ , Cu ₂ MgO ₃	–	CuO, MgAl ₂ O ₄ , Cu ₂ MgO ₃	[65]
CuO, MgAl ₂ O ₄ , Cu ₂ MgO ₃ , SrAl ₂ O ₄	–	CuO, MgAl ₂ O ₄ , Cu ₂ MgO ₃ , SrAl ₂ O ₄	
CuO, MgAl ₂ O ₄ , Cu ₂ MgO ₃ , BaAl ₂ O ₄	–	CuO, MgAl ₂ O ₄ , Cu ₂ MgO ₃ , SrAl ₂ O ₄	
Fe ₂ O ₃ , CaSO ₄	CaO, CaS, Ca ₂ FeO ₃ Cl	CaSO ₄ , CaCl ₂ , Ca ₂ FeO ₃ Cl	[57]
Fe ₂ O ₃ /Al ₂ O ₃	Fe ₂ O ₃ , Al ₂ O ₃ , Fe ₃ O ₄	–	[24, 108]
CaO decorated Fe ₂ O ₃ /Al ₂ O ₃	Fe ₂ O ₃ , Al ₂ O ₃ , Fe ₃ O ₄ , CaO, CaOSiO ₂ , Ca ₂ Fe ₂ O ₃ , SiO ₂	–	
Cu ₄ Al ₆	CuAl ₂ O ₄ , CuO, Cu ₂ O, Al ₂ O ₃ , Cu	CuAl ₂ O ₄ , CuO, Al ₂ O ₃	[25]
Fe ₄ Al ₆	Fe ₂ O ₃ , Al ₂ O ₃ , Fe ₃ O ₄	Fe ₂ O ₃ , Al ₂ O ₃	
Iron ore with 5%K (AEM)	–	Fe ₂ O ₃ , K ₃ FeO ₂ , KAlSiO ₄	[64]
Iron ore with 15%K (AEM)	KFeCl ₃ , K ₂ TiCl ₆ , KAlCl ₂ O, KCl, Fe ₃ O ₄ , FeO	K ₂ Fe ₂₃ O ₃₄ , Fe ₂ O ₃	
Iron ore with 5%Na (AEM)	–	NaAlSiO ₄ , Na ₃ Fe ₉ O ₃₆ , Fe ₂ O ₃	
Iron ore with 15%Na (AEM)	NaCl, Fe ₃ O ₄ , FeO	Fe ₂ O ₃ , Na _{0.9} (Fe _{0.9} Si _{0.1})O ₂ , NaAlSiO ₄	
Iron ore with 5%Ca (AEM)	–	Fe ₂ O ₃ , CaFe ₂ O ₄	
Iron ore with 15%Ca (AEM)	Ca ₃ Al ₂ (SiO ₄) ₂ Cl ₄ , Ca ₂ SiO ₃ Cl ₂ , Fe ₃ O ₄ , FeO, CaCl ₂ , Fe	Fe ₂ O ₃ , Ca ₂ Fe ₂ O ₅	

reactor. Since this is similar to carbon conversion, the same trend is obtained, and the same factors that affect carbon conversion also affect the conversion rate.

Phase characterization

Since the oxygen carrier gets re-oxidized and reduced for several cycles when MSW is introduced into the reactor, there is a need to characterize and compare the oxygen carrier before and after the completion of the CLC experiment. This will determine if a new organic compound is absorbed by the oxygen carrier, which might affect the reactivity of the oxygen carrier. The X-ray diffraction (XRD) analysis indicates the active components present in the solid sample. This can also be used to determine if there are ash deposits on the oxygen carrier, which can cause the deactivation of the oxygen carrier [96]. The oxidation and reduction phase of the oxygen carriers obtained from the XRD analysis is summarized in Table 3.

The AEM-modified iron ore oxygen carrier XRD showed a conversion from Fe_2O_3 to Fe_3O_4 and FeO after the reduction of the pure iron oxide. The fresh AEM oxides observed in the fresh oxygen carrier disappeared after ten reduction cycles, and AEM ferrites were formed due to the mixture of the AEM and the iron oxides. The AEM ferrites showed

superior reactivity in chemical looping processes, which was ascribed to the large amount of lattice oxygen associated with Fe [97]. However, the AEM aluminates were stable for both reduced and oxidized states. Hence, a similar XRD was observed. For the CaSO_4 oxygen carrier analyzed by Bi et al. [54], the CaSO_4 was the only component observed from the XRD before the CLC process, and the reduced form of the oxygen carrier contains CaS and CaSiO_3 . For Na, K, and Ca decorated natural iron ore oxygen carriers used to determine the dechlorination performance of CLC of PVC, different K, Na and Ca chlorides were observed after the fifth redox cycle, which would eventually decompose to form Cl_2 when exposed to the atmosphere. The dechlorination products signify a good dechlorination efficiency. However, the presence of $\text{Ca}_3\text{Al}_2(\text{SiO}_4)_2\text{Cl}_4$ and $\text{Ca}_2\text{SiO}_3\text{Cl}_2$ indicated that as the reaction progressed, part of Ca tended to form inert substances with Si/Al in the oxygen carrier and lost its dechlorination ability [55]. The crystalline chlorides were not detected after several redox cycles for the oxygen carriers with high chlorine plastic samples, probably due to low contents or amorphous structures [67]. The XRD analysis of the oxygen carrier of a mixture of CuO , MgO , Al_2O_3 and BaCO_3 or SrCO_3 , which was used for the CLC of syngas derived from MSW [67], is presented in Fig. 4. The calcination of the mixture resulted in the production of the

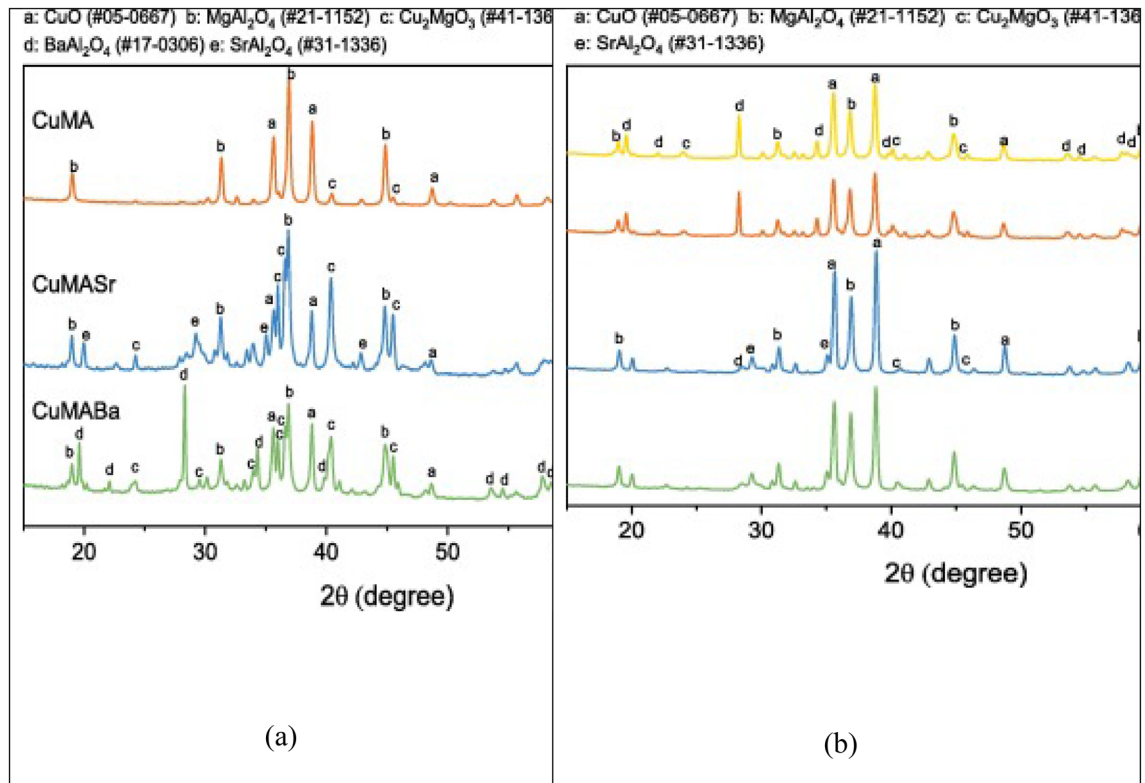


Fig. 4 Phase composition of **a** XRD pattern of fresh Cu-Mg–Al-Br/Sr oxygen carrier **b** XRD pattern after five and 20 cycles [67]

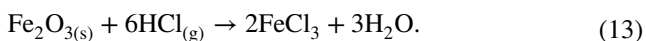
different organic compounds observed (Fig. 4a). Comparing the XRD analysis of the different oxygen carrier composites with the ones obtained after 5 and 20 cycles showed some peaks nearly disappearing (Fig. 4b). The reduction in the Cu_2MgO_3 peak could result from the migration of Cu to the surface of the solid sample during the redox cycles, which led to the uneven distribution of Cu/CuO and limited the dissolution of CuO into the complex oxide Cu_2MgO_3 [98].

Impurities and ash from CLC of MSW

The CLC technology, owing to its carbon capture abilities, has significantly contributed to the reduction in greenhouse gas emissions, making the process more environmentally friendly [78]. For CLC of MSW, chlorine [92], dioxins, heavy metals and sulfur emissions [20] were studied [55]. Since plastic waste was mostly studied, chlorination efficiency and the effect of oxygen carriers on intermediate products of dioxins such as chlorine, HCl and chlorobenzene were analyzed.

HCl, Cl and PCDD/F's emission

PCDD/Fs are formed in all thermal processes when chlorine, oxygen, hydrogen and carbon are present [99]. Chlorine (Cl), which can form acidic pollutants, is the key element in the formation of dioxins, with PVC plastic waste being the primary Cl source in MSW [100]. The dioxin can be inhibited by suppressing the deacon reaction, which can be inhibited by suitable oxygen carriers, temperature or amount of steam. The interaction between HCl present in MSW and iron ore (Fe_2O_3) was analyzed to mimic a CLC process, and the effect of steam on the chlorine gas quantity produced during the reduction process was investigated. The amount of chlorine was measured using a methyl orange spectrophotometric method described by Zhang et al. [86]. At a CLC temperature of between 700 and 900 °C, increasing the amount of steam added to the CLC process was found to reduce the amount of chlorine gas produced [86]. The oxygen carrier was also found to absorb the HCl with iron chloride gas formed at this temperature based on Eq. 13. The use of $\text{CaSO}_4/\text{Fe}_2\text{O}_3$ was also found to absorb the HCl present in PVC plastic waste to produce $\text{Ca}_2\text{FeO}_3\text{Cl}$, as seen in the XRD in Figure f. However, the formation of this $\text{Ca}_2\text{FeO}_3\text{Cl}$ indicated a decreased regeneration of the $\text{CaSO}_4/\text{Fe}_2\text{O}_3$ oxygen carrier [56].



Dechlorination efficiency was analyzed when K, Na, and Ca decorated iron ore was used as an oxygen carrier for

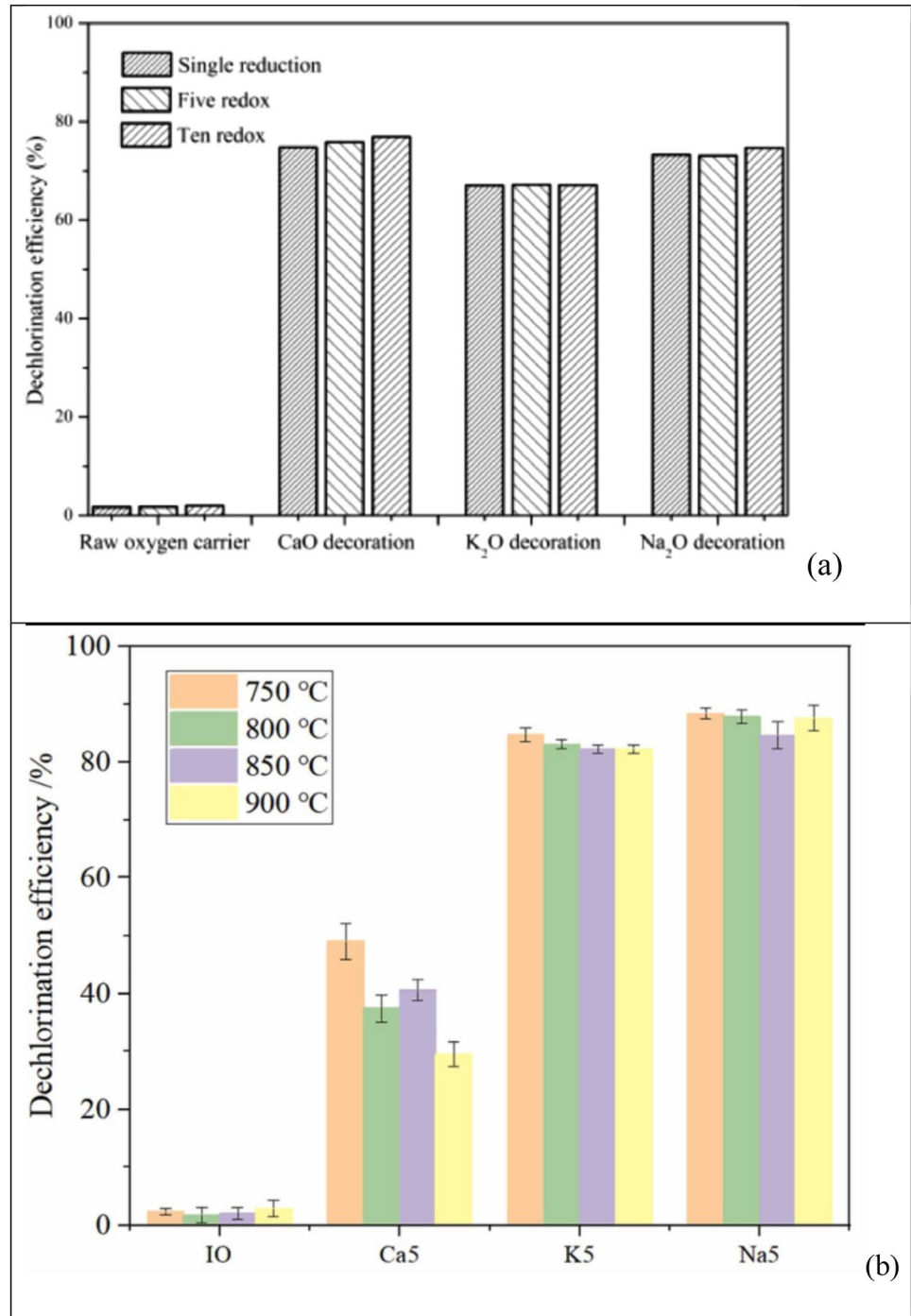
medical and PVC plastic waste. This was calculated as a measure of the ratio of the flue gas's total chlorine content to chlorine's total molar content in the plastic waste, which was measured using an ion chromatograph. The three decorated iron ore oxygen carriers analyzed with the medical plastic waste showed a dechlorination efficiency greater than 65%, with CaO-decorated iron ore having the highest dechlorination efficiency [92]. However, for the PVC plastic, CaO had the lowest dichlorination efficiency at 45%. Among the three decorated iron ores analyzed, CaO was found to have the highest activation energy during its reaction with the HCl gas from the synthetic pyrolysis gas. This led to a lower reaction rate and hence a lower dechlorination efficiency, as obtained by Jiang et al. [55] (See Fig. 5).

It is believed that the significant difference between the dichlorination efficiency of CaO decorated and NaO and KO could be that from the reaction with HCl, CaCl_2 had a substantially higher volume than KCl and NaCl produced from the same quantity of HCl, which promoted its buildup on the OC's surface after synthesis and hampered HCl diffusion to its interior pores. Wang and Zhao [92] also believed that the close chlorination efficiency obtained with the medical plastic waste was due to the intrinsic reactivity of adsorbent with HCl, the mass and heat transfer under the atmosphere of fluidized bed reactor and physical properties such as surface area and pore structure when these adsorbents were decorated with $\text{Fe}_2\text{O}_3/\text{Al}_2\text{O}_3$ OC particles. Also, increasing the temperature from 850 to 925 °C favored the dechlorination efficiency. However, this led to the decomposition of methane, which resulted in the deposition of more carbon (less combustion efficiency). Like the $\text{CaSO}_4/\text{Fe}_2\text{O}_3$ oxygen carrier, the decorated oxygen carrier regeneration ability decreases as the redox cycle increases for both dechlorination efficiency research papers [55, 92]. This has led to up to a 65% reduction in dechlorination efficiency after about 30 redox cycles [92]. As observed in Table 1, the chlorine present in the plastic waste gets absorbed by the AEM oxides after several cycles, resulting in a reduced regeneration ability.

Furthermore, a detailed thermodynamics analysis of the chlorine interaction with iron oxide and ilmenite showed a high concentration of HCl. Comparing the two oxygen carriers, iron oxide produced a lower HCl concentration, while ilmenite produced a large amount of HCl. As seen in [55, 56, 92], using modified iron ore was found to reduce the HCl concentrations. However, this led to the production of calcium and alkali chlorides which led to the formation of slag that causes corrosion of the bed material.

In summary, CLC can potentially reduce the formation of dioxins in chlorine containing MSW such as PVC, compared to pyrolysis, as analyzed by Bi et al. [54]. Moreover, modified oxygen carriers have a better dichlorination efficiency than single oxygen carriers. On the other hand, modified

Fig. 5 a Dechlorination efficiency of different modified oxygen carriers **b** Dechlorination efficiency of different oxygen carriers at different temperatures



oxygen carriers promote the production of alkali chlorides on the reactor bed, which not only decreases the oxygen carrier's regenerative potential but also causes bed material degradation.

Alkali interactions with oxygen carriers

Common alkali and alkali earth metals present in high concentrations in MSW ash are Ca, K and Na [101]. During the

CLC process, these metals can react with silicates present in some oxygen carriers or in the ash, forming alkali silicates in the form of vicious melts and binding the bed particles together. This can lead to bed agglomeration and defluidization [102]. Less work has been done on analyzing different oxygen carriers used with MSW and their interactions with its ash. Stanicic et al. [103] discussed in detail the interactions of the alkalis in MSW ash with ilmenite and iron oxide carriers. The authors discovered that fewer alkali chlorides

(KCl and NaCl) are produced with ilmenites than iron oxide. K_2O and Na_2O are also formed for both oxygen carriers but in small quantities and tend to reduce with an increase in ash content. Also, as explained in the previous section, a high amount of potassium aluminate silicates is produced with iron oxides ($K_2Al_2Si_4O_{12}$) and ilmenite ($KAlSi_3O_8$). $KAlSiO_4$, observed in the XRD phase characterization of the AEM-modified iron ore with MSW syngas [55], was also observed from the thermodynamic calculation in relatively smaller quantities. For Na, $NaAlSiO_4$ at high concentration is observed with $KAlSi_3O_8$ in minimal concentrations. In summary, it can be seen that both K and Na do not interact identically with oxygen carriers, and the potassium aluminum silicate is majorly in the leucite and feldspar phase, while that of sodium aluminum silicate is in the nepheline phase [103].

Heavy metals interactions with oxygen carriers

MSW contains a relatively high amount of heavy metals that are highly harmful to the natural environment and human health compared to other solid fuels (coal and biomass) [104]. In addition to the common alkali and alkaline earth metal compounds, studies have shown that the combustion of waste-derived fuels in fluidized bed boilers may increase trace elements in the fly ashes [105]. As a result, heavy metal emissions are one of the CLC's challenges and concerns.

FactSage 5.3.1 software was used to calculate the equilibrium distributions of heavy metals during the chemical looping gasification of MSW by Cai et al. [106]. The authors explored the transformation and migration of heavy metals such as Pb, Cd, Zn, Cr, and Cu in calcium-based CLG using the optimal operating condition of Ca-CLG (equivalence ratio (ER) of 1.2, a mass ratio of steam to carbon (S/C) of 2, and a mass ratio of calcium to carbon (Ca/C) of 2). The authors concluded that with the exception of Pb, the other heavy metals could be stabilized into solid compounds during gasifier operation temperature of 600–750 °C. Pb, however, could convert into solid sulfides if sulfur was present in the MSW. The distribution of Pb is similar to what was observed by Stancic et al. [63].

The fate of Zinc, Copper and Lead during oxygen-aided combustion was also studied by Stancic et al. [107], with ilmenite as an oxygen carrier. Four MSW ash samples were characterized, and it was discovered that iron on the surface of ilmenite particles interacts with copper and zinc present in the MSW fly ash to form ferrites, $CuFe_2O_4$ and $ZnFe_2O_4$. Lead, however, ended up as condensed $PbCl_2$ in the fly ash, but mixed oxide $PbTiO_3$ was identified at the oxygen carrier surface. Although the oxygen carrier has been able to absorb the metals from the ash, this reduces the oxygen carrier's reactivity and life span. However, these Pb, Zn and Cu compounds were slightly different from what was obtained

from the fact stage thermodynamic database calculation, as expected. More of Zn_2SiO_4 and less of $ZnFe_2O_4$ was obtained, $Cu_5FeS_4Cu_2O$ and Cu solids were obtained with copper and PbS, Pb, PbO gas and Pb(s) and $Pb_2FeSi_2O_7$ at high ash concentration of about 20–60% in the MSW.

Several phases of chlorides, alkali and heavy metal interactions were presented based on experimental characterization and thermodynamic calculations. Dissimilar results were expected in some cases due to the limitations in software calculations, such as isothermal conditions. However, an important thing to note is the formation of chlorides due to the high chlorine present in MSW which can lead to the formation of dioxins, a toxic pollutant and a high amount of alkali silicates which can lead to corrosion and fouling of bed materials.

However, Chen et al. [20] introduced an innovation by combining CLC and CLG in order to remove the heavy metals absorbed by the oxygen carrier. Cadmium (Cd), primarily distributed in fly ash due to the generation of the reducing gas during CLG based on copper and iron-based oxygen carriers, was used to test the process. The concentration of cadmium in the OC particles grew linearly with the number of cycles, from 7.1 mg/kg of MSW to 33.3 mg/kg, with an average capture efficiency of 85%. In contrast, the high concentration of cadmium in the OC particles could be removed efficiently after just one cycle of the CLG process. The implication of this additional unit operation in terms of cost and profitability needs to be explored.

Modeling and simulation of CLC of MSW

Design, optimization, and scale-up efforts benefit from mathematical modeling of the reduction and oxidation reactions inside CLC reactors. CLC simulation primarily involves reactor fluid dynamics, reaction scheme, reaction kinetics (changing grain size model, shrinking core model, nucleation and nuclei growth models), reactor residence time distribution, and process simulation [108]. Because of its extensive physical and thermodynamic property data banks and fully developed modules, the Advanced System for Process Engineering (ASPEN Plus®) is widely used in CLC simulation. However, Chemcad software has also been used for simulation for MSW [58] and other solid fuels such as coal [109] and biomass [110].

Hua and Wang [61] compared the performance of a CLC MSW process with conventional MSW incineration to determine the deacon reaction activity with different oxygen carriers. This was analyzed using ASPEN plus software, and the thermodynamic analysis reveals that the amount of Cl_2 oxidized by the seven oxygen carriers studied in the deacon reaction is less than that oxidized by air. The results also showed that the activity of lattice oxygen in the deacon

reaction is lower than that of molecular oxygen. Two types of CLC processes (IG-CLC and CLOU) were analyzed by Yaqub et al. [58] with MSW and compared with coal. Chemcad software was used to predict their performances and the process simulation demonstrated that using MSW has a solid fuel in CLC and has an equal (IG-CLC) and better (CLOU) CO₂ capture efficiency and combustion efficiency than coal. The MSW (waste paper and plastics) was also blended, and the results showed that the IG-CLC process had a higher CO₂ yield (higher degree of CO₂ capture) than the CLOU process (30–80 percent) for the individual waste paper and plastic waste samples and the waste paper/plastic blends [64]. The CLOU process had marginally higher combustion efficiencies for all the different waste plastics and paper than the IG-CLC process. In comparison, the IG-CLC process had higher combustion efficiency (30–75 percent) for blends than the CLOU process (25–70 percent).

However, it was observed that only process simulation has been used to predict the performance of CLC had been done for MSW. Numerical simulation, reactor modeling, the reaction kinetics of oxygen carriers and computational fluid dynamics are lacking for MSW fuel. This is necessary in order to characterize the system's fluidization and chemical kinetics [111] and can be used in the future to develop guidelines for optimal unit operation [31].

Challenges and future outlook

The general key challenge faced with the CLC of solid fuels is the incomplete conversion of char in the fuel reactor. This leads to a high concentration of unreacted char in the bed of the fuel reactor [43]. This results in the unreacted char being circulated together with the oxygen carrier to the air reactor, which reduces the CO₂ capture rate. Solutions such as the introduction of a secondary fuel reactor were proposed by Gayan et al. [112]. Other solutions were proposed, such as reducing the interaction between the ash from solid fuels and oxygen carriers by magnetic separation [113].

However, one major challenge for MSW is the interaction between oxygen carriers and MSW ashes during prolonged exposure. This has been found to lead to the deactivation of oxygen carriers due to agglomeration, attrition and carbon deposits [96]. Hence, the focus should be on ash content on the type of solid fuel, optimum experimental conditions and oxygen carrier composition in order to minimize these challenges [114]. Since the ash is usually deposited on the oxygen carrier, separating ash from the oxygen carrier is another challenge, and this separation's effectiveness has received little attention. Also, tar formation must be extensively researched, especially from plastic waste produced during pyrolysis. This is because the undesired tar can clog, foul, and corrode downstream pipes [115]. Also, studies on

phosphorus interaction with oxygen carriers have not been well analyzed. Although, compared to coal and biomass, MSW has a smaller phosphorus concentration, and most XRD analysis has not been able to identify phosphorus compounds in the oxygen carrier [62, 63].

While CLC has been found to be a promising technology in converting waste to energy, research on finding optimal conditions to minimize emission levels and maximize combustion performance needs to be prioritized. Pilot-scale chemical looping process demonstrations can serve as essential foundations for the future of MSW chemical looping processes. Further research should include combining the kinetic data of MSW with the fuel and air reactors, which will allow the design of reactors optimized for the MSW conversion and dynamic simulations of the CLC system.

While using the different reactors has shown positive results, some limitations were observed with some of the reactors. These limitations are, however, not specific to MSW samples. For interconnected fluidized bed reactors, gas leakages usually occur between the fuel and the air reactor [116]. This can be minimized by connecting another fuel reactor which serves as a carbon stripper, and a loop seal that connects the carbon stripper to the air reactor [43]. This has been implemented in a 50 kWth CLC unit by Ma et al. [117]. Also, the bubbling bed fuel reactor was found to have a little gas-solids reaction due to the low solids circulation rate [118]. This challenge was overcome by increasing solid inventory in the fuel reactor [42]. It is believed that these solutions can also be considered for the CLC-MSW process.

Furthermore, it is critical to conduct research to improve the adaptability of oxygen carriers (long-life oxygen carriers), while maintaining reactivity and structural integrity over multiple redox cycles. More importantly, focusing on the economic conversion of MSW to high-value chemical products and liquid fuels would hasten the commercialization of the MSW CLC process on a large scale. Although Mohn et al. [119] investigated the economic potential of converting waste to energy with CLC, additional experimental calculation needs to be implemented in order to determine the feasibility of the process such as revenue from the negative emissions of biogenic components of MSW. Additionally, research on the CLOU of MSW needs to be studied. Compared to iG-CLC, there is a significant difference in the degree of development of this process.

Finally, these challenges mentioned above have made the commercialization of the CLC of MSW difficult. To proceed with upscaling, total confidence in the oxygen carrier employed for the CLC of MSW must be established.

Conclusion

MSW is an important energy source; further research into its conversion to energy will reduce our reliance on fossil fuels. Given its carbon neutrality, significant environmental benefits are expected as this can provide clean, renewable energy solutions to reduce net GHG emissions. As discussed in this review, the CLC of MSW has received a lot of attention, because it has the potential for providing a sustainable path to decarbonized energy and management of MSW. The performance of CLC of different MSW types was reviewed, and this conversion pathway has been found to be a promising technology.

Different types of MSW reviewed in this manuscript include plastic waste (polyvinylchloride (PVC), polyethylene, polyurethane, polypropylene, polyethylene terephthalate, polystyrene, high-density polyethylene and low-density polyethylene), waste paper, MSW blends (waste paper and different plastics), a mixture combustible MSW, inert materials and non-combustible MSW to represent actual MSW and MSW-derived syngases. From the different types of reactor configurations used for CLC of MSW (annular dual-type moving bed reactor, dual batch fluidized bed, semi-continuously operated fluidized bed, two-staged pipe reactor, gas-switching fluidized bed reactor, fixed bed reactor system and fluidized bed reactor), the fluidized bed reactor is the most often utilized reactor configuration because it is easy to obtain high and homogeneous solid–gas mass transfer.

Suitable oxygen carriers such as AEM-modified oxygen carriers have been found to be ideal for reducing the quantity of HCl produced, thereby reducing dioxin emissions. Also, improved combustion efficiency and increasing carbon conversion were obtained using modified oxygen carriers compared to single oxygen carriers. The challenge of ash interaction with oxygen carriers and the phase characterization of different oxygen carriers before and after CLC experiments was presented. The XRD analysis performed on the oxygen carrier showed that the deposits of some of the heavy metals from MSW ash affect the combustion efficiency and dichlorination efficiency due to its deactivation after several cycles and can induce corrosion and fouling of bed materials. The development of better oxygen carriers that can maintain reactivity after several cycles and the economic feasibility of the system need to be studied in the future.

Funding Open access funding provided by University of Johannesburg.

Open Access This article is licensed under a Creative Commons Attribution 4.0 International License, which permits use, sharing, adaptation, distribution and reproduction in any medium or format, as long as you give appropriate credit to the original author(s) and the source, provide a link to the Creative Commons licence, and indicate if changes

were made. The images or other third party material in this article are included in the article's Creative Commons licence, unless indicated otherwise in a credit line to the material. If material is not included in the article's Creative Commons licence and your intended use is not permitted by statutory regulation or exceeds the permitted use, you will need to obtain permission directly from the copyright holder. To view a copy of this licence, visit <http://creativecommons.org/licenses/by/4.0/>.

References

1. Nikku M, Deb A, Sermyagina E, Puro L (2019) Reactivity characterization of municipal solid waste and biomass. *Fuel*. <https://doi.org/10.1016/j.fuel.2019.115690>
2. Sipra AT, Gao N, Sarwar H (2018) Municipal solid waste (MSW) pyrolysis for bio-fuel production: a review of effects of MSW components and catalysts. *Fuel Process Technol* 175:131–147
3. Rasmeni Z, Madyira D (2019) A review of the current municipal solid waste management practices in Johannesburg City Townships. *Sustain Mater Process Manuf* 35:1025–1031
4. Ng WPQ, Lam HL, Varbanov PS, Klemeš JJ (2014) Waste-to-energy (WTE) network synthesis for municipal solid waste (MSW). *Energy Convers Manag* 85:866–874
5. Rizwan M, Saif Y, Almansoori A, Elkamel A (2019) Environmental performance of municipal solid waste processing pathways. *Energy Procedia* 158:3363–3368
6. Seadon JK (2010) Sustainable waste management systems. *J Clean Prod* 18(16–17):1639–1651
7. Diaz LF (2017) Waste management in developing countries and the circular economy. *Waste Manag Res* 35(1):1–2
8. Singh A (2014) Groundwater resources management through the applications of simulation modeling: a review. *Sci Total Environ* 499:414–423
9. Alavi Moghadam MR, Mokhtarani N, Mokhtarani B (2009) Municipal solid waste management in Rasht City, Iran. *Waste Manag* 29(1):485–489
10. Le Courtois A (2012) Municipal solid waste: turning a problem into resource. *Priv Sect Dev* 15:1–28
11. Hla SS, Roberts D (2015) Characterisation of chemical composition and energy content of green waste and municipal solid waste from Greater Brisbane, Australia. *Waste Manag* 41:12–19
12. Mahad B, Abdullah A-M, Hamid O, Wala A-A (2017) Ultimate composition analysis of municipal solid waste in Muscat. *J Clean Prod* 148:355–362
13. Lu JW, Zhang S, Hai J, Lei M (2017) Status and perspectives of municipal solid waste incineration in China: a comparison with developed regions. *Waste Manag* 69:170–186
14. Rudra S, Tesfagaber YK (2019) Future district heating plant integrated with municipal solid waste (MSW) gasification for hydrogen production. *Energy* 180:881–892
15. Buekens A (2013) Evaluation of waste incineration. *Springer Briefs Appl Sci Technol*. https://doi.org/10.1007/978-1-4614-5752-7_2
16. Gabbar HA, Aboughaly M, Ayoub N (2018) Comparative study of MSW heat treatment processes and electricity generation. *J Energy Inst* 91(4):481–488
17. Wang P, Hu Y, Cheng H (2019) Municipal solid waste (MSW) incineration fly ash as an important source of heavy metal pollution in China. *Environ Pollut* 252:461–475
18. Tian H, Gao J, Lu L, Zhao D, Cheng K, Qiu P (2012) Temporal trends and spatial variation characteristics of hazardous air pollutant emission inventory from municipal solid waste incineration in China. *Environ Sci Technol* 46(18):10364–10371

19. Wang J, Zhao H (2016) Evaluation of CaO-decorated Fe₂O₃/Al₂O₃ as an oxygen carrier for in-situ gasification chemical looping combustion of plastic wastes. *Fuel* 165:235–243
20. Chen P, Sun X, Gao M, Ma J, Guo Q (2019) Transformation and migration of cadmium during chemical-looping combustion/gasification of municipal solid waste. *Chem Eng J*. <https://doi.org/10.1016/j.cej.2019.02.041>
21. Leion H, Mattisson T, Lyngfelt A (2007) The use of petroleum coke as fuel in chemical-looping combustion. *Fuel* 86(12–13):1947–1958
22. Khan R, Patel V (2021) “The Influence of global climate change on freshwater ecosystem,” in *Water Conservation in the Era of Global Climate Change* pp. 347–366
23. Cheng W et al (2022) Global monthly gridded atmospheric carbon dioxide concentrations under the historical and future scenarios. *Sci. Data* 9(1):83
24. Ströhle J (2023) Chemical looping combustion of waste—opportunities and challenges. *Energy Fuels*. <https://doi.org/10.1021/acs.energyfuels.2c04297>
25. Lewis WK, Gilliland ER (1954) “Production of Pure Carbon Dioxide”
26. Adanez J, Abad A, Garcia-Labiano F, Gayan P, De Diego LF (2012) Progress in chemical-looping combustion and reforming technologies. *Prog Energy Combust Sci* 38(2):215–282
27. Adánez J, Abad A (2019) Chemical-looping combustion: status and research needs. *Proc Combust Inst* 37(4):4303–4317
28. Wang X, Liu X, Zhang Y, Zhang B, Jin B (2019) Numerical investigation of solid-fueled chemical looping combustion process utilizing char for carbon capture. *Processes*. <https://doi.org/10.3390/pr7090603>
29. Lin J, Luo K, Sun L, Wang S, Hu C, Fan J (2019) Numerical investigation of nickel-copper oxygen carriers in chemical-looping combustion process with zero emission of CO and H₂. *Energy Fuels* 33(11):12096–12105
30. Nandy A, Loha C, Gu S, Sarkar P, Karmakar MK, Chatterjee PK (2016) Present status and overview of chemical looping combustion technology. *Renew Sustain Energy Rev* 59:597–619
31. Adánez J, Abad A, Mendiara T, Gayán P, de Diego LF, García-Labiano F (2018) Chemical looping combustion of solid fuels. *Prog Energy Combust Sci* 65:6–66
32. Abad A, Adánez-Rubio I, Gayán P, García-Labiano F, de Diego LF, Adánez J (2012) Demonstration of chemical-looping with oxygen uncoupling (CLOU) process in a 1.5kWth continuously operating unit using a Cu-based oxygen-carrier. *Int J Greenh Gas Control* 6:189–200
33. Mei D, Abad A, Zhao H, Adánez J (2015) Characterization of a sol-gel derived CuO/CuAl₂O₄ oxygen carrier for chemical looping combustion (CLC) of gaseous fuels: relevance of gas-solid and oxygen uncoupling reactions. *Fuel Process Technol* 133:210–219
34. Leion H, Mattisson T, Lyngfelt A (2009) Using chemical-looping with oxygen uncoupling (CLOU) for combustion of six different solid fuels. *Energy Procedia* 1(1):447–453
35. Gu H, Shen L, Zhang S, Niu M, Sun R, Jiang S (2018) Enhanced fuel conversion by staging oxidization in a continuous chemical looping reactor based on iron ore oxygen carrier. *Chem Eng J* 334:829–836
36. Pérez-Vega R et al (2018) Chemical looping combustion of gaseous and solid fuels with manganese-iron mixed oxide as oxygen carrier. *Energy Convers Manag* 159:221–231
37. Ma J, Tian X, Wang C, Chen X, Zhao H (2018) Performance of a 50 kWth coal-fuelled chemical looping combustor. *Int J Greenh Gas Control* 75:98–106
38. Cormos CC (2015) Biomass direct chemical looping for hydrogen and power co-production: Process configuration, simulation, thermal integration and techno-economic assessment. *Fuel Process Technol* 137:16–23
39. Yaqub ZT, Oboirien BO, Hedberg M, Leion H (2021) Experimental evaluation using plastic waste, paper waste, and coal as fuel in a chemical looping combustion batch reactor. *Chem Eng Technol* 44(6):1075–1083
40. Moldenhauer P, Rydén M, Mattisson T, Jamal A, Lyngfelt A (2017) Chemical-looping combustion with heavy liquid fuels in a 10 kW pilot plant. *Fuel Process Technol* 156:124–137
41. Xiao R, Chen L, Saha C, Zhang S, Bhattacharya S (2012) Pressurized chemical-looping combustion of coal using an iron ore as oxygen carrier in a pilot-scale unit. *Int J Greenh Gas Control* 10:363–373
42. Lyngfelt A, Linderholm C (2017) Chemical-looping combustion of solid fuels—status and recent progress. *Energy Procedia* 114:371–386
43. Song T, Shen L (2018) Review of reactor for chemical looping combustion of solid fuels. *Int J Greenh Gas Control* 76:92–110
44. Adánez J, Abad A, Perez-Vega R, der Diego LF, García-Labiano F, Gayán P (2014) Design and operation of a coal-fired 50 kWth chemical looping combustor. *Energy Procedia* 63:63–72
45. Linderholm C, Lyngfelt A (2015) Chemical-looping combustion of solid fuels. In: Fennell P, Anthony B (eds) *Calcium and chemical looping technology for power generation and carbon dioxide (CO₂) capture*, 1st edn. Woodhead Publishing, pp 299–326
46. Cao Y et al (2005) Reduction of Solid Oxygen Carrier (CuO) by Solid Fuel (coal) in Chemical Looping Combustion, Preprints of Symposia - American Chemical Society. *Div Fuel Chem* 50(1):99–102
47. Gupta P, Velazquez-Vargas LG, Thomas T, Fan L-S (2005) “Chemical looping combustion of coal to produce hydrogen,” in *Proceedings of the International Technical Conference on Coal Utilization & Fuel Systems*, 30(1): 349–352
48. Cheng M, Sun H, Li Z, Cai N (2017) Annular carbon stripper for chemical-looping combustion of coal. *Ind Eng Chem Res* 56(6):1580–1593
49. Fan LS (2010) *Chemical looping particles. Chemical looping systems for fossil energy conversions*. Wiley, pp 57–142
50. Cao Y, Casenas B, Pan WP (2006) Investigation of chemical looping combustion by solid fuels. 2. Redox reaction kinetics and product characterization with coal, biomass, and solid waste as solid fuels and CuO as an oxygen carrier. *Energy Fuels* 20(5):1845–1854
51. Gu H, Shen L, Xiao J, Zhang S, Song T (2011) Chemical looping combustion of biomass/coal with natural iron ore as oxygen carrier in a continuous reactor. *Energy Fuels* 25(1):446–455
52. Thunman H, Lind F, Breitholtz C, Berguerand N, Seemann M (2013) Using an oxygen-carrier as bed material for combustion of biomass in a 12-MWth circulating fluidized-bed boiler. *Fuel* 113:300–309
53. Corcoran A, Marinkovic J, Lind F, Thunman H, Knutsson P, Seemann M (2014) Ash properties of ilmenite used as bed material for combustion of biomass in a circulating fluidized bed boiler. *Energy Fuels* 28(12):7672–7679
54. Bi W, Zhao R, Chen T, Wu J, Wu J (2015) Study on the formation of PCDD/Fs in PVC chemical looping combustion. *J Fuel Chem Technol* 43(7):884–889
55. Jiang H et al (2022) Dechlorination performance in chemical looping conversion of polyvinyl chloride plastic waste using K/Na/Ca-modified iron ore oxygen carriers. *J Environ Chem Eng*. <https://doi.org/10.1016/j.jece.2022.107314>
56. Bi W, Chen T, Zhao R, Wang Z, Wu J, Wu J (2015) Characteristics of a CaSO₄ oxygen carrier for chemical-looping combustion: reaction with polyvinylchloride pyrolysis gases in a two-stage reactor. *RSC Adv* 5(44):34913–34920

57. Chiu PC, Ku Y, Wu HC, Kuo YL, Tseng YH (2014) Chemical looping combustion of polyurethane and polypropylene in an annular dual-tube moving bed reactor with iron-based oxygen carrier. *Fuel* 135:146–152
58. Yaqub ZT, Oboirien BO, Akintola AT (2021) Process modeling of chemical looping combustion (CLC) of municipal solid waste. *J Mater Cycles Waste Manag.* <https://doi.org/10.1007/s10163-021-01180-0>
59. Zhao L et al (2016) Characterization of Singapore RDF resources and analysis of their heating value. *Sustain Environ Res* 26(1):51–54
60. Ma J, Wang J, Tian X, Zhao H (2019) In-situ gasification chemical looping combustion of plastic waste in a semi-continuously operated fluidized bed reactor. *Proc Combust Inst* 37(4):4389–4397
61. Hua X, Wang W (2015) Chemical looping combustion: a new low-dioxin energy conversion technology. *J Environ Sci* 32:135–145
62. Wang H et al (2021) Iron ore modified with alkaline earth metals for the chemical looping combustion of municipal solid waste derived syngas. *J Clean Prod.* <https://doi.org/10.1016/j.jclepro.2020.124467>
63. Staničić I, Backman R, Cao Y, Rydén M, Aronsson J, Mattisson T (2022) Fate of trace elements in oxygen carrier aided combustion (OCAC) of municipal solid waste. *Fuel.* <https://doi.org/10.1016/j.fuel.2021.122551>
64. Yaqub Z, Oboirien B (2020) Process modelling of chemical looping combustion of paper, plastics, paper/plastic blend waste, and coal. *ACS Omega* 5(35):22420–22429
65. Hakandai C, Sidik Pramono H, Aziz M (2022) Conversion of municipal solid waste to hydrogen and its storage to methanol. *Sustain Energy Technol Assessments.* <https://doi.org/10.1016/j.seta.2022.101968>
66. Leckner B, Mattisson T, Lyngfelt A (2001) A fluidized-bed combustion process with inherent CO₂ separation; application of chemical-looping combustion. *Chem Eng Sci* 56(10):3101–3113
67. Liu G et al (2022) Thermal behavior of Cu-Mg-Al-Ba/Sr bifunctional composites during chemical looping combustion and HCl adsorption of MSW syngas. *Chem Eng J.* <https://doi.org/10.1016/j.cej.2021.132871>
68. Zhao H, Wang J (2018) Chemical-looping combustion of plastic wastes for in situ inhibition of dioxins. *Combust Flame* 191:9–18
69. Wang H, Liu G, Veksha A, Giannis A, Lim TT, Lisak G (2021) Effective H₂S control during chemical looping combustion by iron ore modified with alkaline earth metal oxides. *Energy.* <https://doi.org/10.1016/j.energy.2020.119548>
70. Hossain MM, de Lasa HI (2008) Chemical-looping combustion (CLC) for inherent CO₂ separations—a review. *Chem Eng Sci* 63(18):4433–4451
71. Chisalita DA, Cormos AM (2018) Dynamic simulation of fluidized bed chemical looping combustion process with iron based oxygen carrier. *Fuel* 214:436–445
72. Tong A, Kathe MV, Wang D, Fan L-S (2018) The moving bed fuel reactor process. *Handbook of chemical looping technology.* Wiley, pp 1–40
73. Miyahira K, Aziz M (2022) Hydrogen and ammonia production from low-grade agricultural waste adopting chemical looping process. *J Clean Prod.* <https://doi.org/10.1016/j.jclepro.2022.133827>
74. Yan J, Shen L, Jiang S, Wu J, Shen T, Song T (2017) Combustion performance of sewage sludge in a novel CLC system with a two-stage fuel reactor. *Energy Fuels* 31(11):12570–12581
75. Tong A, Bayham S, Kathe MV, Zeng L, Luo S, Fan LS (2014) Iron-based syngas chemical looping process and coal-direct chemical looping process development at Ohio State University. *Appl Energy* 113:1836–1845
76. Chen L, Yang L, Liu F, Nikolic HS, Fan Z, Liu K (2017) Evaluation of multi-functional iron-based carrier from bauxite residual for H₂-rich syngas production via chemical-looping gasification. *Fuel Process Technol* 156:185–194
77. Berdugo Vilches T, Lind F, Rydén M, Thunman H (2017) Experience of more than 1000 h of operation with oxygen carriers and solid biomass at large scale. *Appl Energy* 190:1174–1183
78. Lyngfelt A (2020) Chemical looping combustion: status and development challenges. *Energy Fuels* 34(8):9077–9093
79. Shafiefarhood A, Stewart A, Li F (2015) Iron-containing mixed-oxide composites as oxygen carriers for chemical looping with oxygen uncoupling (CLOU). *Fuel* 139:1–10
80. Mohammad Pour N, Leion H, Rydén M, Mattisson T (2013) Combined Cu/Mn oxides as an oxygen carrier in chemical looping with oxygen uncoupling (CLOU). *Energy Fuels* 27(10):6031–6039
81. Källén M, Hallberg P, Rydén M, Mattisson T, Lyngfelt A (2014) Combined oxides of iron, manganese and silica as oxygen carriers for chemical-looping combustion. *Fuel Process Technol* 124:87–96
82. Dudek RB, Tian X, Blivin M, Neal LM, Zhao H, Li F (2019) Perovskite oxides for redox oxidative cracking of n-hexane under a cyclic redox scheme. *Appl Catal B Environ* 246:30–40
83. Song T, Zheng M, Shen L, Zhang T, Niu X, Xiao J (2013) Mechanism investigation of enhancing reaction performance with CaSO₄/Fe₂O₃ oxygen carrier in chemical-looping combustion of coal. *Ind Eng Chem Res* 52(11):4059–4071
84. Mattisson T, Lyngfelt A, Leion H (2009) Chemical-looping with oxygen uncoupling for combustion of solid fuels. *Int J Greenh Gas Control* 3(1):11–19
85. Jiang J (2005) Solid waste disposal Project 99(9)
86. Zhang J, Dong C, Wang L, Yang Y (2009) “The interaction between HCl and Fe₂O₃ during the chemical looping combustion of MSW,” 1st Int. Conf. Sustain. Power Gener. Supply, SUPER-GEN '09
87. Li F, Zeng L, Velazquez-Vargas LG, Yoscovits Z, Fan LS (2010) Syngas chemical looping gasification process: bench-scale studies and reactor simulations. *AIChE J* 56(8):2186–2199
88. Pérez-Astray A et al (2020) Improving the oxygen demand in biomass CLC using manganese ores. *Fuel.* <https://doi.org/10.1016/j.fuel.2020.117803>
89. Pérez-Vega R, Abad A, García-Labiano F, Gayán P, de Diego LF, Adánez J (2016) Coal combustion in a 50 kWth chemical looping combustion unit: seeking operating conditions to maximize CO₂ capture and combustion efficiency. *Int J Greenh Gas Control* 50:80–92
90. Boon YZ (2020) Oxygen carriers for the chemical looping combustion of MSW syngas and HCl removal. Retrieved from <https://hdl.handle.net/10356/138734>
91. Liu G et al (2022) Effect of alkali earth metal doping on the CuO/Al₂O₃ oxygen carrier agglomeration resistance during chemical looping combustion. *J Clean Prod* 366:132970
92. Wang J, Zhao H (2015) Chemical looping dechlorination through adsorbent-decorated Fe₂O₃/Al₂O₃ oxygen carriers. *Combust Flame.* <https://doi.org/10.1016/j.combustflame.2015.06.008>
93. Qasim M, Ayoub M, Ghazali NA, Aqsha A, Ameen M (2021) Recent advances and development of various oxygen carriers for the chemical looping combustion process: a review. *Ind Eng Chem Res* 60(24):8621–8641
94. Liu W, Lim JY, Saucedo MA, Hayhurst AN, Scott SA, Dennis JS (2014) Kinetics of the reduction of wüstite by hydrogen

- and carbon monoxide for the chemical looping production of hydrogen. *Chem Eng Sci* 120:149–166
95. Aljerf L (2015) Effect of thermal-cured hydraulic cement admixtures on the mechanical properties of concrete. *Inter-ceram Int Ceram Rev* 64(8):346–356
 96. Staničić I, Brorsson J, Hellman A, Mattisson T, Backman R (2022) Thermodynamic analysis on the fate of ash elements in chemical looping combustion of solid fuels—iron-based oxygen carriers. *Energy Fuels*. <https://doi.org/10.1021/acs.energyfuels.2c01578>
 97. Huang F et al (2019) Fe-substituted Ba-hexaaluminate with enhanced oxygen mobility for CO₂ capture by chemical looping combustion of methane. *J Energy Chem*. <https://doi.org/10.1016/j.jechem.2018.02.003>
 98. Recio A, Liew S, Lu D, Rahman R, Macchi A, Hill J (2016) The effects of thermal treatment and steam addition on integrated CuO/CaO chemical looping combustion for CO₂ capture. *Technologies* 4(2):11
 99. Altarawneh M, Długogorski BZ, Kennedy EM, Mackie JC (2009) Mechanisms for formation, chlorination, dechlorination and destruction of polychlorinated dibenzo-p-dioxins and dibenzofurans (PCDD/Fs). *Prog Energy Combust Sci* 35(3):245–274
 100. Watanabe N, Yamamoto O, Sakai M, Fukuyama J (2004) Combustible and incombustible speciation of Cl and S in various components of municipal solid waste. *Waste Manag* 24(6):623–632
 101. Wang L et al (2017) Characterization of ash deposits from municipal solid waste (MSW) incineration plants. *Energy Procedia* 142:630–635
 102. Gatternig B, Karl J (2015) Investigations on the mechanisms of ash-induced agglomeration in fluidized-bed combustion of biomass. *Energy Fuels* 29(2):931–941
 103. Staničić I, Brorsson J, Hellman A, Mattisson T, Backman R (2022) Thermodynamic analysis on the fate of ash elements in chemical looping combustion of solid fuels—iron-based oxygen carriers. *Energy Fuels* 36(17):9648–9659
 104. Wienchol P, Szłęk A, Ditaranto M (2020) Waste-to-energy technology integrated with carbon capture—challenges and opportunities. *Energy*. <https://doi.org/10.1016/j.energy.2020.117352>
 105. Backman R, Hupa M, Hiltunen M, Peltola K (2005) “Interaction of The behavior of lead and zinc with alkalis in fluidized bed combustion or gasification of waste derived fuels,” *Proc. 18th Int. Conf. Fluid. Bed Combust.* 2005, pp. 651–659
 106. Cai J, Zheng W, Luo M, Kuang C, Tang X (2021) Characterization of copper (II) chemical forms and heavy metal distribution in chemical looping gasification of municipal solid waste. *J Energy Inst* 96:140–147
 107. Staničić I, Mattisson T, Backman R, Cao Y, Rydén M (2021) Oxygen carrier aided combustion (OCAC) of two waste fuels—experimental and theoretical study of the interaction between ilmenite and zinc, copper and lead. *Biomass Bioenergy*. <https://doi.org/10.1016/j.biombioe.2021.106060>
 108. Abad A, Adánez J, García-Labiano F, de Diego LF, Gayán P (2010) Modeling of the chemical-looping combustion of methane using a Cu-based oxygen-carrier. *Combust Flame* 157(3):602–615
 109. Nguyen NM, Alobaid F, Dieringer P, Epple B (2021) Biomass-based chemical looping gasification: overview and recent developments. *Appl Sci*. <https://doi.org/10.3390/app11157069>
 110. Bhui B, Vairakannu P (2019) Prospects and issues of integration of co-combustion of solid fuels (coal and biomass) in chemical looping technology. *J Environ Manag* 231:1241–1256
 111. Banerjee S, Agarwal RK (2017) Review of recent advances in process modeling and computational fluid dynamics simulation of chemical-looping combustion. *Int J Energy Clean Environ* 18(1):1–37
 112. Gayán P, Abad A, de Diego LF, García-Labiano F, Adánez J (2013) Assessment of technological solutions for improving chemical looping combustion of solid fuels with CO₂ capture. *Chem Eng J* 233:56–69
 113. Abián M et al (2017) Titanium substituted manganese-ferrite as an oxygen carrier with permanent magnetic properties for chemical looping combustion of solid fuels. *Fuel* 195:38–48
 114. Bao J, Li Z, Cai N (2014) Interaction between iron-based oxygen carrier and four coal ashes during chemical looping combustion. *Appl Energy* 115:549–558
 115. Fan Y et al (2020) Minimizing tar formation whilst enhancing syngas production by integrating biomass torrefaction pretreatment with chemical looping gasification. *Appl Energy*. <https://doi.org/10.1016/j.apenergy.2019.114315>
 116. Lindmüller L, Haus J, Ramesh Kumar Nair A, Heinrich S (2022) Minimizing gas leakages in a system of coupled fluidized bed reactors for chemical looping combustion. *Chem Eng Sci*. <https://doi.org/10.1016/j.ces.2021.117366>
 117. Ma J, Zhao H, Niu P, Chen X, Tian X, Zheng C (2016) “Design and Operation of a 50 kWth Chemical Looping Combustion (CLC) Reactor Using Coal as Fuel,” 1: 1–11
 118. Markström P, Linderholm C, Lyngfelt A (2013) Chemical-looping combustion of solid fuels—design and operation of a 100kW unit with bituminous coal. *Int J Greenh Gas Control* 15:150–162
 119. Mohn P, Hofmann C, Alobaid F, Strohle J, Epple B (2022) “Application of Chemical Looping Combustion on Waste-to-Energy: A Techno-Economic Assessment,” in 16th International Conference on Greenhouse Gas Control Technologies, GHGT-16
 120. USA EPA, “National Overview: Facts and Figures on Materials, Wastes and Recycling.” [Online]. Available: www.epa.gov/facts-and-figures-about-materials-waste-and-recycling/national-overview-facts-and-figures-materials. Accessed 19 Sep 2019

Publisher's Note Springer Nature remains neutral with regard to jurisdictional claims in published maps and institutional affiliations.